

Programmable design of soft pneu-net actuators with oblique chambers can generate coupled bending and twisting motions

Tianyu Wang^{a,b,1}, Lisen Ge^{a,c,1}, Guoying Gu^{a,c,*}

^a State Key Laboratory of Mechanical System and Vibration, Shanghai Jiao Tong University, Shanghai 200240, China

^b University of Michigan-Shanghai Jiao Tong University Joint Institute, Shanghai Jiao Tong University, Shanghai 200240, China

^c Robotics Institute, School of Mechanical Engineering, Shanghai Jiao Tong University, Shanghai 200240, China



ARTICLE INFO

Article history:

Received 20 September 2017

Received in revised form 6 January 2018

Accepted 8 January 2018

Available online 10 January 2018

Keywords:

Soft pneumatic actuator

Pneu-net actuator

Coupled bending and twisting motion

Finite element analysis

Dexterous grasping

ABSTRACT

Soft pneumatic network (pneu-net) actuators are widely employed for achieving sophisticated motions. However, to produce bending and twisting simultaneously in a single pneu-net actuator is challenging. In this paper we present a programmable design to enable pneu-net actuators to achieve such complex motions. This achievement is mainly owing to tuning a structure parameter, the chamber angle. Through finite element analysis and experimental verification, variation trends of bending and twisting motions with respect to the chamber angle are investigated. Additionally, deformation characteristics of actuators are demonstrated by depicting configurations of actuators and some grasping tests. By adjusting the chamber angle, the motion of pneu-net actuators is explored into 3-D space and becomes more sophisticated and dexterous. This programmable design method guides the design of pneu-net actuators, making them promising candidates for more complicated and advanced applications.

© 2018 Elsevier B.V. All rights reserved.

1. Introduction

Different from the traditional robots generally for repetitive works with specific environments, soft robots are emerging with the capabilities of large shape deformation for the adaptive and compatible interactions with the environments [1–4]. During the last decade, extensive soft robots have been developed that can realize grasping [5], manipulating [6], creeping [7], crawling [8], swimming [9], and jumping motions [10]. The actuators for soft robots are commonly constructed from compliant materials, such as silicones [6], shape memory polymers [11], shape memory alloys [12], electroactive polymers [13] and hydrogels [14]. Diverse stimuli such as pressurized fluids [7], heats [11,12], electric fields [13] and chemical reactions can be utilized to drive the actuators [10]. Among them, soft pneumatic actuators (SPAs) are more promising in various applications owing to their superiorities of a wide range of motions under simple inputs, lightweight, low material cost, and high fabrication efficiency [14–18].

In abundant designs of SPAs, pneumatic network (pneu-net) actuators [17,19–23] and fiber-reinforced actuators [14,16,24–28] are two popular categories. A fiber-reinforced actuator is mainly

composed of an elastomer body with a monolithic chamber, helically arranged fibers and an alternative inextensible layer [16]. By varying the fiber angles, fiber-reinforced actuators can achieve extension, expanding, bending, and twisting motions [14,25]. Pneu-net actuators are characterized by their multiple connected chambers, functioned as networks [17,23]. As internally pressurized, the chambers of a pneu-net actuator are inflated, and the actuator achieves extension motions. By adding a stiffer layer to limit the extension of the bottom side, the pneu-net actuator realizes bending motions with large amplitudes.

Apart from elementary motion modes in 2-D space, for soft pneumatic actuators, realizing coupled bending and twisting motions in 3-D space is important for more dexterous operations [14,24,29–32]. To bend and twist simultaneously, a fiber-reinforced actuator may employ several families of fibers with various angles. As an early attempt, Hirai et al. [31,32] proposed an analytical basis and demonstrated those motions using deformable cylindrical actuators. They also realized compound actions with pneumatic group actuators, which composed of multiple single-motion elastic tubes. Moser et al. [27,28] applied an analytical model and created a snake-like fiber-reinforced actuator by parallel combining fibers and employing an additional fiber. Connolly et al. [14,24] analyzed in detail how the motion of fiber-reinforced actuators was affected by the fiber angle and raised an analytical model for fast design. Sun et al. [18] offered an alternative method to achieve helical movements by circumferentially shifting every step of the strain-constraining layer of a soft pneumatic actuator. Corre-

* Corresponding author at: State Key Laboratory of Mechanical System and Vibration, Shanghai Jiao Tong University, Shanghai 200240, China.

E-mail address: guguoying@sjtu.edu.cn (G. Gu).

¹ These authors contributed equally to this work.

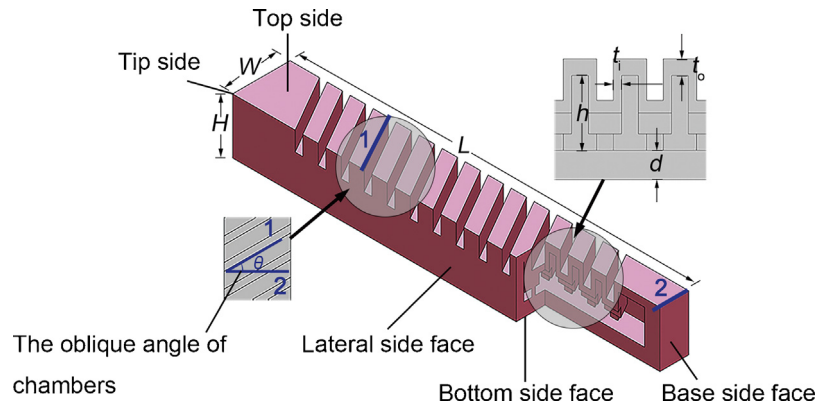


Fig. 1. The structure of a pneu-net actuator with oblique chambers.

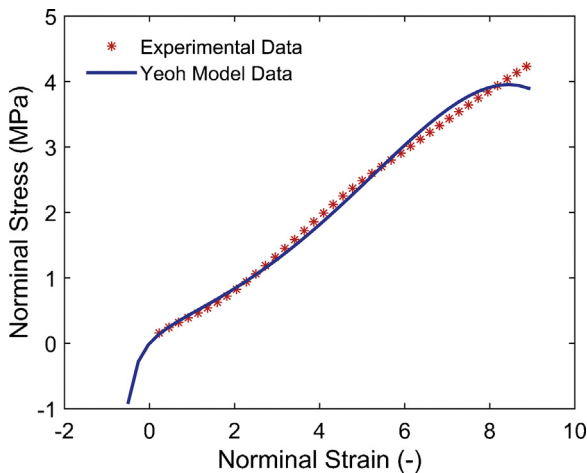


Fig. 2. The stress-strain curve for the silicone Elastosil M4601 based on experimental test data and theoretical model data. The test nominal stress-strain data of each specimen is fitted in ABAQUS with the Yeoh model. Since this model still results in excessive deformation and causes a convergence problem, an extra fitting process is conducted to overcome this problem. The coefficients of the model are finally determined as $C10=0.125$ and $C20=0.0075$.

spondingly, a pneu-net actuator should employ oblique chambers to realize coupled bending and twisting motions. Ilievski et al. [5] firstly developed an embedded network of channels design for a finger, which, when actuated, curled in a helix. Gorissen et al. [33] developed a pure twisting actuator, by combining two opposite bending motions, each of which was realized by a group of angular voids. Although pneu-net actuators' bending and twisting motions have been observed in previous works, there is still lack of study to analyze how the chamber angle affects this motion.

In this paper, we present a programmable design of pneu-net actuators that can generate coupled bending and twisting motions by tuning the chamber angle. We numerically and experimentally investigate the influences of chambers' orientation on the actuator's deformation and motion. The fabrication process follows the simple molding method as other pneu-net actuators [23]. The motions of actuators with varied chamber angles can be predicted by the finite element analysis (FEA). Based on the FEA results, we can adjust chamber angles of the actuator to generate a wide range of deformations. To verify the development, we fabricate actuators with 30° , 45° , 60° oblique chambers and conduct a series of experiments. Experimental results of the relationship between the motion of actuators and the chamber angle agree well with the FEA simulation results. Tests on grasping objects with different sizes and shapes (such as tubes, cylinder, scissors, and Ping-Pong ball) demonstrate that the fabricated actuator can realize a more

stable grasping with a sufficient contact area and better adaptability towards different geometric features of target objects. We show our programmable design method based on simulations and experiments could guide the design of pneu-net actuators for more applications.

2. Materials and methods

The actuator presented in this paper is based on the prevalent pneu-net actuators which are comprised of elastomeric materials with multiple connected chambers, functioned as pneumatic networks [17,23]. The previous research and analysis upon pneu-net actuators are mostly focusing on their bending property in two-dimensional space [17,23]. Here, we present a new structure of pneu-net actuators that generates coupled bending and twisting motions in three-dimensional space by modifying the angle of the pneu-net chamber. We define the chamber angle as θ , as shown in Fig. 1. The orientation of chambers in Mosadegh's structure [17] is perpendicular to the long edge of the actuator, which naturally means, θ equals to 0 degrees. When the value of θ changes, the deformation will become complicated as the actuators are pressurized. When an actuator is pressurized internally, the thinner inside walls of chambers inflate. The inflation direction is perpendicular to the oblique chambers, resulting in coupled bending and twisting motions in the three dimensions. By programming the chamber angles, we can obtain a more sophisticated actuator for dexterous grasping that is comparable with the programmable fiber-reinforced pneumatic actuators [24]. We will demonstrate later that the motion of the new design is also predictable by the finite element model.

For a pneu-net actuator, there is a set of geometrical parameters (Fig. 1) that influence the performance and behavior of the actuator. And different combinations of these parameters determine a large number of actuators which may have various performances. A lot of works have been done about how some parameters alter actuators' performances like the height of chambers, the wall thickness, and the total length of the actuator [17,23]. In this work, we focus on one specific parameter that has not been exploited, the chamber angle θ , to investigate the behavior of actuators as the chamber angle changes.

To make sure the only changing parameter is the chamber angle, other parameters in experiments are fixed as follow: the total length of the actuator $L = 104$ mm, the width of the actuator $W = 15$ mm, the height of the actuator $H = 14.5$ mm, the height of chambers $h = 5$ mm, the inside wall thickness $t_i = 1$ mm, the outside/top wall thickness $t_o = 2$ mm, and the thickness of the bottom layer $d = 3.5$ mm. The width and total length of the actuator is fixed. According to our design, as the chamber angle increases, the length of each chamber increases and the number of chambers decreases.

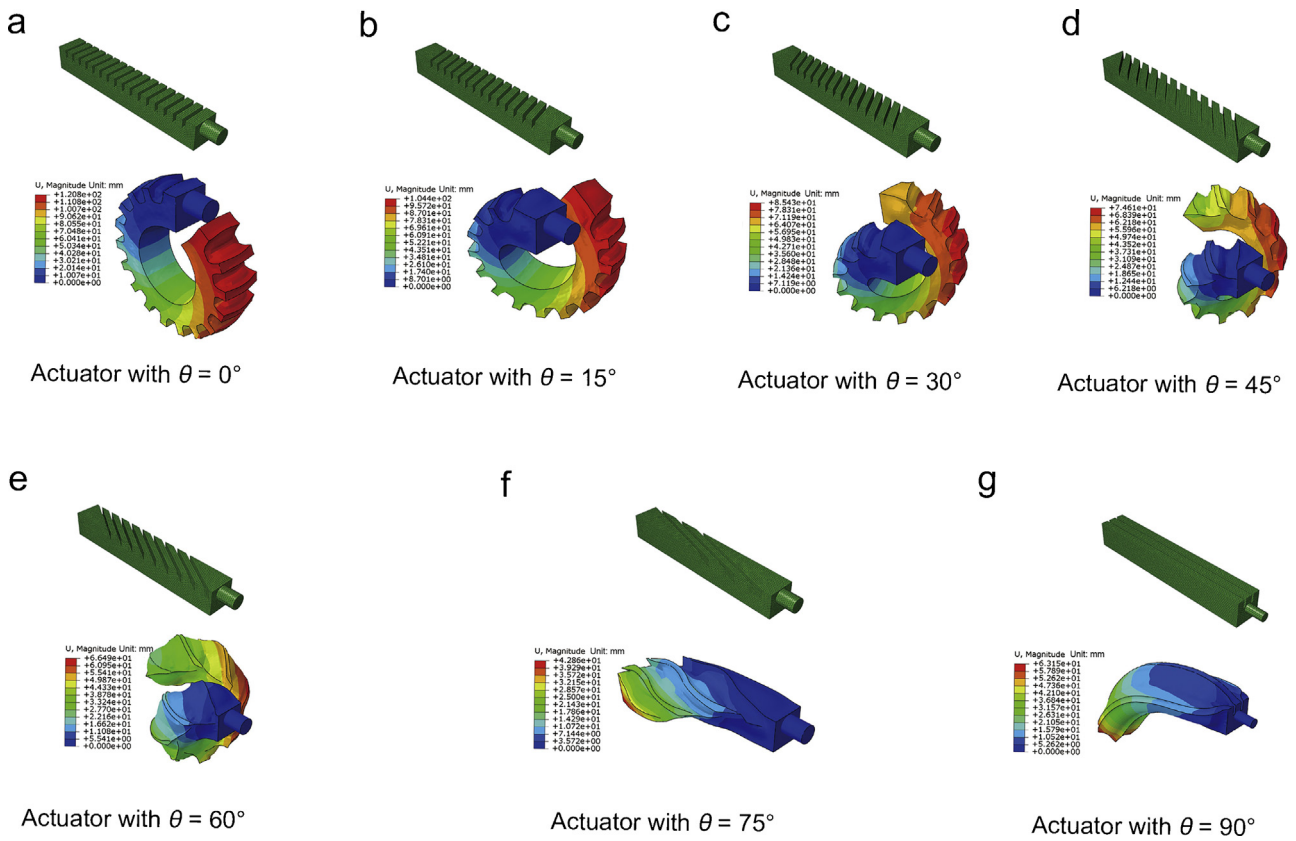


Fig. 3. FEA results of the pneu-net actuators with different θ under the same boundary conditions. The original and deformed shapes of each actuator are demonstrated in (a) - (g).

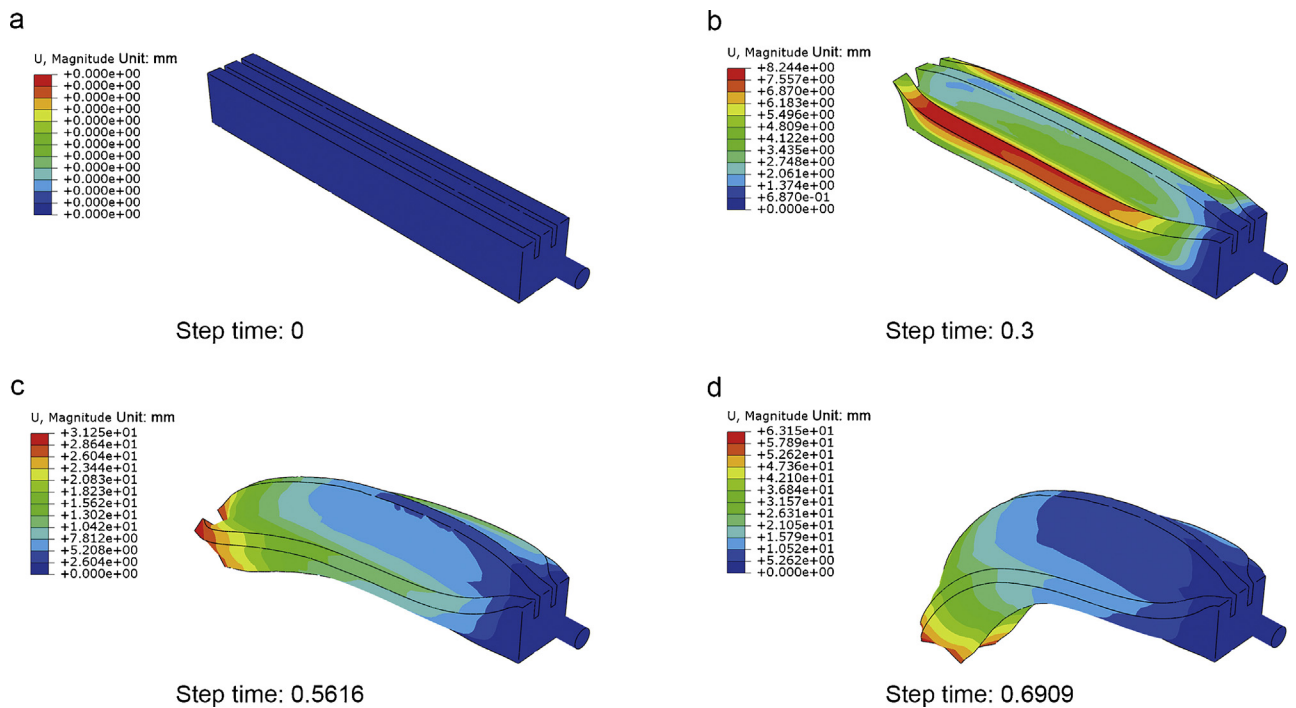


Fig. 4. FEA results of sequential deformation images of the actuator with $\theta = 90^\circ$.

The fabrication process follows a traditional molding method [1,23]. The three-part molds are designed in Solidworks, and 3-D printed out. Two of them are assembled to make the upper part of the actuator, and the other is for the bottom layer. After mixing and

defoaming Elastosil M4601 (Wacker) part A and B, Elastosil M4601 is poured into the molds. When the Elastosil solidifies, molds are removed. Then the upper part and the bottom layer are attached with Elastosil.

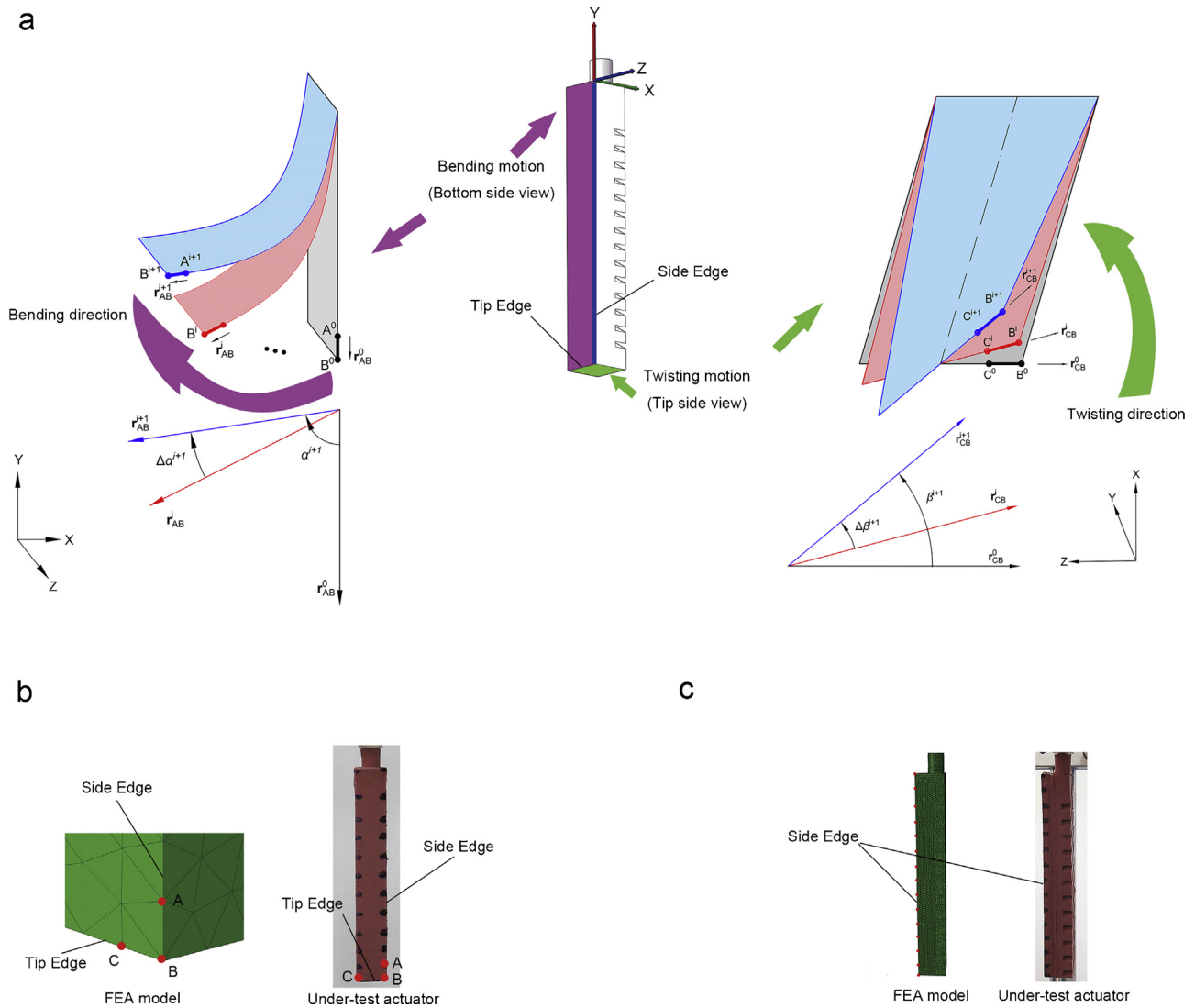


Fig. 5. The illustration of how the bending angle α and twisting angle β of a deformed actuator are extracted and calculated based on the FEA results and experimental results. (a) The actuator's motion is decoupled as a bending motion and a twisting motion. Vector \mathbf{r}_{AB} along Side Edge and vector \mathbf{r}_{CB} along Tip Edge are selected to calculate the bending angle and twisting angle respectively. (b) Node A, B, and C in FEA simulations and in experiments. For convenience, Node C in experiments is not in the same position as that in FEA simulations, since we assume the deformation of Tip edge can be neglected. (c) Markers selected to describe the deformed configuration of Side edge in the FEA simulations and experiments.

3. Results and discussion

A series of finite element analyses were executed to determine the proper chamber angle, θ . The geometry models of the actuators with different values of θ (0° , 15° , 30° , 45° , 60° , 75° , 90°) were designed in SolidWorks 2016 (Dassault Systemes S.A). The models were meshed in HyperMesh 13.0 (Altair) with C3D4H elements. The element size was set as 1 mm. The meshed models were then imported into ABAQUS 6.14-4 (Dassault Systemes S.A) for FEA simulations. Uniaxial tensile tests were executed according to the standard ASTM D638 [23] to determine the constitutive model parameters of the actuator's material (Fig. 2). Gravity and uniformly distributed internal pressure (90 kPa) were applied to the actuators. As shown in Fig. 2, the Yeoh model shows some discrepancies with the silicone Elastosil M4601 test data at large tensile strains and at compressive strains. It should be noted that the Yeoh model is applicable in this work since the deformations of our designed actuators are generally within the range 0–600%, in which this model matches well with the real data.

FEA results of displacement contours for each actuator are demonstrated in Fig. 3. As expected, a pure bending motion appears

when $\theta = 0^\circ$. The chambers expand and the actuator then generates the bending deformation when $\theta = 90^\circ$ (Fig. 4). The other five actuators can generate coupled bending and twisting motions. We can see from the FEA simulation results (Fig. 3) that under the same input pressure, as the chamber angle increases, the actuator's bending motion level decreases and the twisting motion level increases, which can be verified by the following calculation and analysis of bending and twisting angle as shown in Fig. 6.

The motion of this kind of actuators can be decoupled as bending and twisting. To describe the bending and twisting motion, we first elaborate how the bending angle α and twisting angle β are extracted.

As shown in Fig. 5, the vector \mathbf{r}_{AB} is selected to calculate the bending angle of the actuator. We name the vector \mathbf{r}_{AB} as \mathbf{r}_{AB}^i and \mathbf{r}_{AB}^{i+1} at the i -th iteration step and the $i + 1$ -th iteration step respectively. The increment of the bending angle $\Delta\alpha^{i+1}$ from the i -th iteration step to the $i + 1$ -th iteration step is

$$\Delta\alpha^{i+1} = \arccos \frac{\mathbf{r}_{AB}^i \cdot \mathbf{r}_{AB}^{i+1}}{|\mathbf{r}_{AB}^i| |\mathbf{r}_{AB}^{i+1}|}. \quad (1)$$

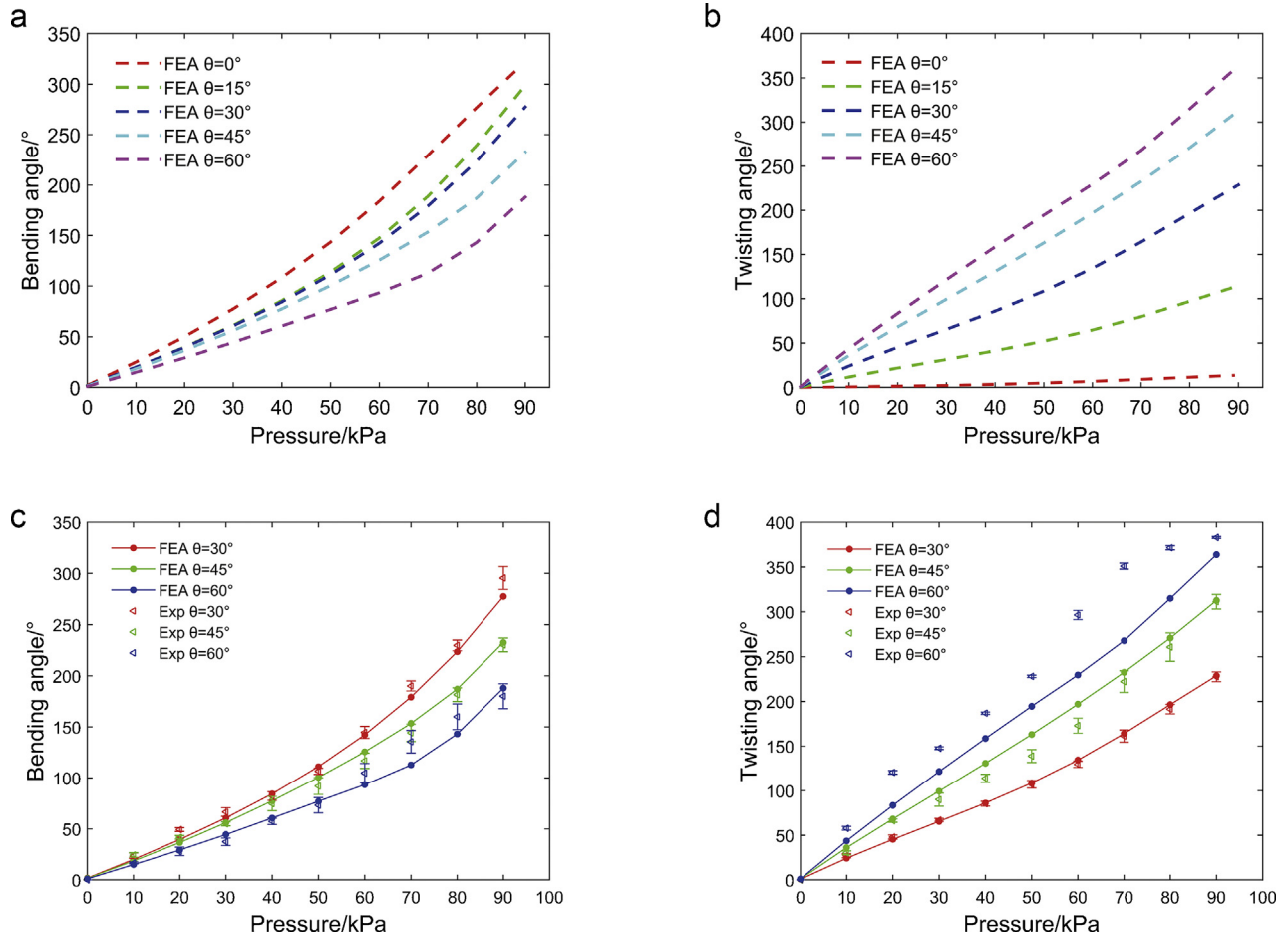


Fig. 6. Bending angles and twisting angles as functions of internal pressures for actuators with different θ . (a) – (b) show FEA results, (c) – (d) show comparisons between FEA results and experimental test results. We choose the three actuators with $\theta = 30^\circ$, $\theta = 45^\circ$, $\theta = 60^\circ$ for the tests. Each actuator is tested three times as the pressure varied from 0 to 90 kPa. The error bars represent the standard deviation from the average result of the three tests.

The accumulative bending angle α^{i+1} as of the $i + 1$ -th iteration step is

$$\alpha^{i+1} = \alpha^i + \Delta\alpha^{i+1}. \quad (2)$$

The method of calculating the twisting angle β is similar to the bending angle α . The vector \mathbf{r}_{CB} is chosen to determine the twisting angle.

The FEA results of bending angles for actuators with different chamber angles are demonstrated in Fig. 6a. The bending angle of each actuator apparently goes up with the increase of the pressure. The actuator’s bending deformation capacity decreases when the chamber angle increases. The actuator with $\theta = 0^\circ$ acquires the maximum bending angle 318° , while the actuator with $\theta = 60^\circ$ deforms with a bending angle of 188° .

Results in Fig. 6b shows the twisting angles of the actuators with oblique chambers goes up with the increase of the pressure. The actuators with larger chamber angle can twist more easily. The actuator with $\theta = 15^\circ$ and $\theta = 60^\circ$ twists to 115° and 364° respectively. It should be noted that the calculation of the twisting angle relies on the vector \mathbf{r}_{CB} . Theoretically, the actuator with $\theta = 0^\circ$ cannot generate twisting motion, vector \mathbf{r}_{CB} should not change and the twisting angle should keep zero. However, vector \mathbf{r}_{CB} would slightly change because of the inflation deformation of the actuator under the input pressure. This tiny increase of inflation deformation caused by the increasing input pressure results in minor positive increments of the calculated twisting angle.

To verify the finite element results, we conducted experiments on the three kinds of actuators with $\theta = 30^\circ$, $\theta = 45^\circ$ and $\theta = 60^\circ$

since we expected they had the best performances according to FEA simulations (see Video 1). We fix the tested actuator on its base side, and let its tip side free to move. To numerically analyze the spatial position of the actuator, we set up a frame (Fig. 5) at the base side of the actuator since the base side will always hold still. We set up a two-camera system to acquire images synchronously. For ease of calculation, one camera’s optical axis is perpendicular to the XY-plane for capturing XY-coordinates, and the other one is perpendicular to the YZ-plane for capturing YZ-coordinates. We took images of the actuator every 10 kPa from 0 to 90 kPa during loading. By tracking markers on the actuator, we could first confirm relative locations for markers on the actuator and reference points in the environment with a software named imageJ (NIH). Relative positions were transformed into 2-D coordinates in Matlab (Math-Works). XY- and YZ-coordinates were combined and processed to produce 3-D coordinates. With 3-D reconstructions of the coordinates of the actuator, we can estimate the bend angle, twist angle and depict configurations under specific pressures.

With the method above, we estimated the bending angle α and the twisting angle β as functions of pressure. (Fig. 6c and d) show the results. The experimental results match well with simulation results: under the same pressure, bending angle α decreases as chamber angle θ increases. It reveals that pure bending capability of actuators can be weakened by increasing the chamber angle. The experimental results also show a good consistency with FEA results on the twisting angle: pure twisting becomes more significant as chamber angle θ increases. However, experimental results cannot match the FEA results perfectly and there exist discrepancies

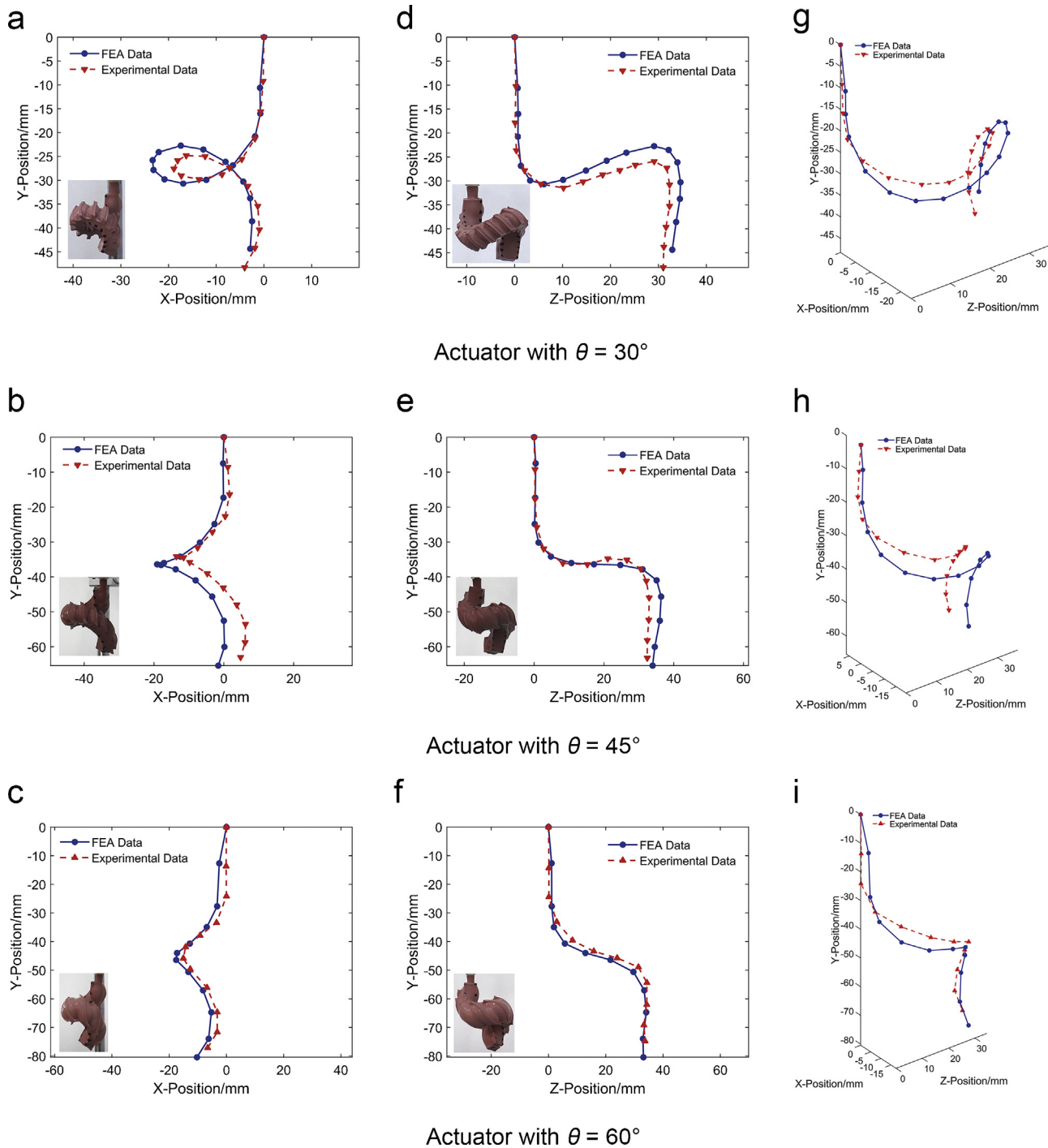


Fig. 7. FEA and experimental test results of the configurations of Side Edge for actuators with $\theta = 30^\circ$, $\theta = 45^\circ$, $\theta = 60^\circ$. Each actuator is tested three times and the ones that most matching the corresponding FEA results are demonstrated here. (a) – (f) show the configuration of Side Edge for each actuator is projected to XY-plane and YZ-plane, (g) – (i) show the configurations of Side Edge in the 3-D space for the three actuators.

between them, as generally reported in the literature [14,16,23,25]. Inconsistencies may come from flaws in fabricating process, instability of the air source, changes in material behaviors after repeated stretching, errors in image processing and locating of markers.

For further studying the deformation of the actuator with different θ under particular conditions, we fixed the internal pressure as 90 kPa and observed configuration of the actuator body. To depict the configuration, we monitor the profile of the Side Edge (Fig. 5). As pressurized, the tip side of the actuator goes towards $-x$, $-y$, $+z$ direction (with the frame set up in Fig. 5). The configuration of each

actuator's Side Edge can be reconstructed by tracking several markers on Side Edge. 2-D configurations in XY-plane, YZ-plane and 3-D configurations of each actuator are shown in Fig. 7.

The actuators sustain an internal pressure of 90 kPa. The comparison in each figure shows that the FEA results agree well with the experimental test results, though some small discrepancies exist. Comparative results show that each of the three actuators can realize coupled bending and twisting motions. The actuator with a larger chamber angle curls up to an approximate helix with a smaller radius of curvature but a larger pitch. In contrast, the body

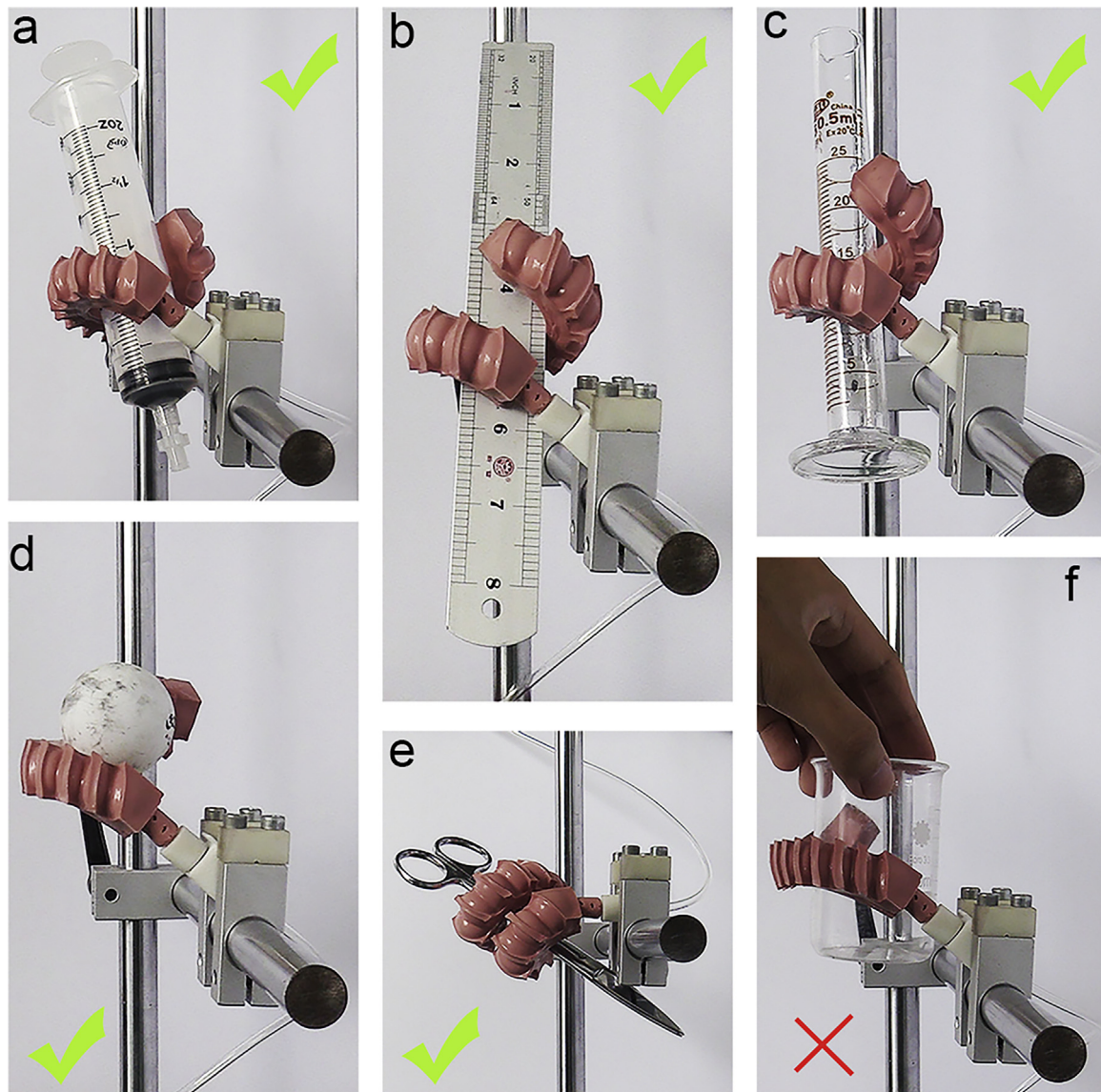


Fig. 8. Grasp experiments for the actuator with $\theta = 30^\circ$. The target objects are (a) a 60 ml syringe, (b) a 20 cm long flat steel ruler, (c) a 25 ml graduated cylinder, (d) a Ping-Pong ball, (e) a slender scissors, and (f) a 100 ml beaker. Experiments in (a) – (e) are succeeded, while the experiment in (f) is failed.

of the actuator with a smaller chamber angle forms a helix with a larger radius of curvature but a smaller pitch. These conclusions on the bending angle, the twisting angle and configurations can give us a great help to design actuators with different characteristics.

Furthermore, we performed a series of dexterous grasping tests to verify the capability of the designed actuators to realize the coupled bending and twisting motions (see Video 2). In this test, the actuator with $\theta = 30^\circ$ was employed as an illustration. Fig. 8 shows the experimental results to grasp different objects, such as syringes, rulers, measuring cylinders, Ping-Pong balls, and scissors. We observe from the experiments that the actuator realizes coupled bending and twisting motions and generates a helical configuration. We can adjust the actuator's helical configuration to fit with target objects with different characteristics by changing the internal pressure. The helical configuration helps the actuator accomplish stable grasping by providing sufficient frictions with larger contact areas and show an excellent adapting capability towards the objects that may not be handled by a single bending pneu-net actuator. However, the grasping capability of the actuator is limited by its body length. Fig. 8f shows a failure of holding a beaker. These

tests prove that the actuators with oblique chambers can generate coupled bending and twisting motions. Benefited from coupled bending and twisting motions, the pneu-net actuators with oblique chambers can perform a more stable and dexterous grasping.

4. Conclusions

This paper presents a programmable design of pneu-net actuators that can generate a wide range of coupled bending and twisting motions by simply tuning a structure parameter, the chamber angle. Effect of chamber angles on the actuators' deformation and motion is analyzed in detail. In finite element simulations and experiments, we calculate bending and twisting angle for each actuator with oblique chambers under different internal pressures. Results demonstrate that as the chamber angle increases, the actuator's bending capacity decreases and twisting capacity increases. Through studying configurations of actuators and single actuator grasping tests, we demonstrate this coupled motion would enable actuators to accomplish more dexterous manipulations. We conclude our programmable design method could guide the rapid

design of pneu-net actuators, which broadens their applications in soft robotics.

Our future work will try to develop an analytical model for this kind of actuator and use the developed model for new actuator design with the desired trajectory. We believe combining chambers with different chamber angles in a single actuator will produce more motion forms for various application demands and our future work will also focus on this issue.

Conflicts of interest

None.

Acknowledgments

This work was supported by the National Natural Science Foundation of China under Grant 51622506 and the Science and Technology Commission of Shanghai Municipality under Grant 16JC1401000.

Appendix A. Supplementary data

Supplementary material related to this article can be found, in the online version, at doi:<https://doi.org/10.1016/j.sna.2018.01.018>

References

- [1] D. Rus, M.T. Tolley, Design, fabrication and control of soft robots, *Nature* 521 (7553) (2015) 467–475, <http://dx.doi.org/10.1038/nature14543>.
- [2] L. Hines, K. Petersen, G.Z. Lum, M. Sitti, Soft actuators for small-scale robotics, *Adv. Mater.* 29 (2017), 1603483, <http://dx.doi.org/10.1002/adma.201603483>.
- [3] S. Kim, C. Laschi, B. Trimmer, Soft robotics: a bioinspired evolution in robotics, *Trends Biotechnol.* 31 (5) (2013) 287–294, <http://dx.doi.org/10.1016/j.tibtech.2013.03.002>.
- [4] G. Gu, J. Zhu, L. Zhu, X. Zhu, A survey on dielectric elastomer actuators for soft robots, *Bioinspir. Biomim.* 12 (1) (2017), 011003, <http://dx.doi.org/10.1088/1748-3190/12/1/011003>.
- [5] F. Ilievski, A.D. Mazzeo, R.F. Shepherd, X. Chen, G.M. Whitesides, Soft robotics for chemists, *Angew. Chem.* 123 (2011) 1930–1935, <http://dx.doi.org/10.1002/anie.201006464>.
- [6] R. Deimel, O. Brock, A novel type of compliant and Underactuated Robotic hand for dexterous grasping, *Int. J. Rob. Res.* 35 (1–3) (2016) 161–185, <http://dx.doi.org/10.1177/0278364915592961>.
- [7] R.F. Shepherd, F. Ilievski, W. Choi, S.A. Morin, A.A. Stokes, A.D. Mazzeo, et al., Multigait Soft robot, *Proc. Natl. Acad. Sci. U. S. A.* 108 (51) (2011) 20400–20403, <http://dx.doi.org/10.1073/pnas.1116564108>.
- [8] H.T. Lin, G.G. Leisk, B. Trimmer, GoQBot: a caterpillar-inspired soft-bodied rolling robot, *Bioinspiration Biomimetics*. 6 (2) (2011) 026007, <http://dx.doi.org/10.1088/1748-3182/6/2/026007>.
- [9] K. Suzumori, S. Endo, T. Kanda, N. Kato, H. Suzuki, A bending pneumatic rubber actuator realizing soft-bodied Manta swimming robot, *IEEE Int. Conf. Rob. Autom.* 2007 (2007) 4975–4980, <http://dx.doi.org/10.1109/ROBOT.2007.364246>.
- [10] H. Lee, C. Xia, N.X. Fang, First jump of Microgel: actuation speed enhancement by elastic instability, *Soft Matter* 6 (2010) 4342–4345, <http://dx.doi.org/10.1039/C0SM00092B>.
- [11] S. Qi, T. Sarah, S. Tyler, P. Viljar, K. Kwang, O. Il-Kwon, A multiple-shape memory polymer-metal composite actuator capable of programmable control, creating complex 3D motion of bending, twisting, and oscillation, *Sci. Rep.* 6 (2016) 24462, <http://dx.doi.org/10.1038/srep24462>.
- [12] R. Hugo, W. Wei, H. Minwoo, J.Y.K. Thomas, A. Sunghoon, An overview of shape memory alloy-coupled actuators and robots, *Soft Rob.* 4 (1) (2017) 3–15, <http://dx.doi.org/10.1089/soro.2016.0008>.
- [13] G. Kofod, W. Wirges, M. Paajanen, S. Bauer, Energy minimization for self-organized structure formation and actuation, *Appl. Phys. Lett.* 90 (8) (2007), 081916, <http://dx.doi.org/10.1063/1.2695785>.
- [14] F. Connolly, P. Polygerinos, C.J. Walsh, K. Bertoldi, Mechanical programming of soft actuators by varying fiber angle, *Soft Rob.* 2 (1) (2015) 26–32, <http://dx.doi.org/10.1089/soro.2015.0001>.
- [15] J. Paek, I. Cho, J. Kim, Microrobotic Tentacles with spiral bending capability based on shape-engineered elastomeric Microtubes, *Sci. Rep.* 5 (2015), 10768, <http://dx.doi.org/10.1038/srep10768>.
- [16] P. Polygerinos, Z. Wang, J.T.B. Overvelde, K.C. Galloway, R.J. Wood, K. Bertoldi, et al., Modeling of soft fiber-reinforced bending actuators, *IEEE Trans. Rob.* 31 (3) (2015) 778–789, <http://dx.doi.org/10.1109/TRO.2015.2428504>.
- [17] B. Mosadegh, P. Polygerinos, C. Keplinger, S. Wennstedt, R.F. Shepherd, U. Gupta, et al., soft robotics: pneumatic networks for soft robotics that actuate rapidly, *Adv. Funct. Mater.* 24 (2014) 2163–2170, <http://dx.doi.org/10.1002/adfm.201303288>.
- [18] Y. Sun, H.K. Yap, X. Liang, J. Guo, P. Qi, M.H. Ang Jr, et al., Stiffness customization and patterning for property modulation of silicone-based soft pneumatic actuators, *Soft Rob.* 4 (3) (2017) 251–260, <http://dx.doi.org/10.1089/soro.2016.0047>.
- [19] S. Wakimoto, K. Ogura, K. Suzumori, Y. Nishioka, Miniature soft hand with curling rubber pneumatic actuators, *IEEE Int. Conf. Rob. Autom.* 2009 (2009) 556–561, <http://dx.doi.org/10.1109/ROBOT.2009.5152259>.
- [20] Y. Hao, T. Wang, Z. Ren, Z. Gong, H. Wang, X. Yang, et al., Modeling and experiments of a soft robotic gripper in amphibious environments, *Int. J. Adv. Rob. Syst.* 14 (3) (2017), 1729881417707148, <http://dx.doi.org/10.1177/1729881417707148>.
- [21] K.M.D. Payrebrune, O.M. O'Reilly, On constitutive relations for a rod-based model of a pneu-net bending actuator, *Extreme Mech. Lett.* 8 (2016) 38–46, <http://dx.doi.org/10.1016/j.eml.2016.02.007>.
- [22] K.C. Galloway, K.P. Becker, P. Brennan, K. Jordan, L. Stephen, T. Dan, et al., Soft robotic grippers for biological sampling on deep reefs, *Soft Rob.* 3 (1) (2016) 23–33, <http://dx.doi.org/10.1089/soro.2015.0019>.
- [23] P. Polygerinos, S. Lyne, Z. Wang, L.F. Nicolini, B. Mosadegh, G.M. Whitesides, et al., Towards a soft pneumatic glove for hand rehabilitation, *IEEE/RSJ Int. Conf. Intell. Robots Syst.* 2013 (2013) 1512–1517, <http://dx.doi.org/10.1109/IROS.2013.6696549>.
- [24] F. Connolly, C.J. Walsh, K. Bertoldi, Automatic design of fiber-reinforced soft actuators for trajectory matching, *Proc. Natl. Acad. Sci. U. S. A.* 114 (1) (2017) 51–56, <http://dx.doi.org/10.1073/pnas.1615140114>.
- [25] B. Wang, A. Mcdaid, M. Biglari-Abhari, T. Giffney, K. Aw, A bimorph pneumatic bending actuator by control of fiber braiding angle, *Sens. Actuators A Phys.* 257 (2017) 173–184, <http://dx.doi.org/10.1016/j.sna.2017.02.003>.
- [26] M.A. Robertson, H. Sadeghi, J.M. Florez, J. Paik, Soft pneumatic actuator fascicles for high force and reliability, *Soft Rob.* 4 (1) (2017) 23–32, <http://dx.doi.org/10.1089/soro.2016.0029>.
- [27] J. Bishop-Moser, S. Kota, Towards snake-like soft robots: design of fluidic fiber-reinforced elastomeric helical manipulators, *IEEE/RSJ Int. Conf. Intell. Robots Syst.* (2013) 5021–5026, <http://dx.doi.org/10.1109/IROS.2013.6697082>.
- [28] J. Bishop-Moser, G. Krishnan, C. Kim, S. Kota, Design of soft robotic actuators using fluid-filled fiber-reinforced elastomeric enclosures in parallel combinations, *IEEE/RSJ Int. Conf. Intell. Robots Syst.* (2012) 4264–4269, <http://dx.doi.org/10.1109/IROS.2012.6385966>.
- [29] R.V. Martinez, J.L. Branch, C.R. Fish, L. Jin, R.F. Shepherd, R.M. Nunes, et al., Robotic tentacles with three-dimensional mobility based on flexible elastomers, *Adv. Mater.* 25 (2013) 205–212, <http://dx.doi.org/10.1002/adma.201203002>.
- [30] K.Y. Hong, B.W.K. Ang, J.H. Lim, J.C.H. Goh, C.H. Yeow, A fabric-regulated soft robotic glove with user intent detection using EMG and RFID for hand assistive application, *IEEE Int. Conf. Rob. Autom.* (2016) 3537–3542, <http://dx.doi.org/10.1109/ICRA.2016.7487535>.
- [31] S. Hirai, P. Cusin, H. Tanigawa, T. Masui, Qualitative synthesis of deformable cylindrical actuators through constraint topology, *IEEE/RSJ Int. Conf. Intell. Robots Syst.* 1 (2000) 197–202, <http://dx.doi.org/10.1109/IROS.2000.894604>.
- [32] S. Hirai, T. Masui, S. Kawamura, Prototyping pneumatic group actuators composed of multiple single-motion elastic tubes, *IEEE International Conference on Robotics and Automation, 2001 Proceedings 4* (2001) 3807–3812, <http://dx.doi.org/10.1109/ROBOT.2001.933211>.
- [33] B. Gorissen, T. Chishiro, S. Shimomura, D. Reynaerts, M.D. Volder, S. Konishi, Flexible pneumatic twisting actuators and their application to tilting Micromirrors, *Sens. Actuators A Phys.* 216 (3) (2014) 426–431, <http://dx.doi.org/10.1016/j.sna.2014.01.015>.

Biographies

Tianyu Wang is currently an undergraduate student at University of Michigan-Shanghai Jiao Tong University Joint Institute, Shanghai Jiao Tong University. His research is in the development of soft robotics.

Lisen Ge received the B.E. degree in Engineering Structure Analysis and M.S. degree in Vehicle Operation Engineering from Southwest Jiaotong University, Chengdu, China, in 2013 and 2016, respectively. He is currently a Ph.D. candidate at School of Mechanical Engineering, Shanghai Jiao Tong University. His research is in the development of soft robotics.

Guoying Gu received the B.E. degree (with honors) in electronic science and technology, and the Ph.D. degree (with honors) in mechatronic engineering from Shanghai Jiao Tong University, Shanghai, China, in 2006 and 2012, respectively. Dr. Gu was a Visiting Scholar at Concordia University, Montreal, QC, Canada, and National University of Singapore, Singapore. Supported by the Alexander von Humboldt Foundation, he was as a Humboldt Fellow at University of Oldenburg, Oldenburg, Germany. Since October 2012, he has worked at Shanghai Jiao Tong University, where he is currently appointed as an Associate Professor with School of Mechanical Engineering. His research interests include soft robotics, high-precision motion control, soft sensors and actuators. He is the author or co-author of over 60 publications, which have appeared in journals, as book chapters and in conference proceedings. Dr. Gu is a member of the IEEE and ASME. Now Dr. Gu serves as Associate Editor of International Journal of Advanced Robotic Systems. He has also served for several international conferences/symposiums as Chair, Associate Editor or Program Committee Member.